Aeroacoustics Conferences
30 May - 1 June, 2016, Lyon, France
22nd AIAA/CEAS Aeroacoustics Conference

Analyzing Noise Components on Skewed Fans with a Virtual Rotating Microphone Array

Gert Herold*
Brandenburg University of Technology, D-03046 Cottbus, Germany

Florian Zenger†
University of Erlangen-Nuremberg, D-91058 Erlangen, Germany

Ennes Sarradj ‡
Brandenburg University of Technology, D-03046 Cottbus, Germany

This contribution applies a method to detect rotating sound sources on measurements performed on forward and backward skewed fans. Aside from the localization of dominant source mechanisms, spectra of the fan's leading and trailing edges are evaluated at different operating conditions. This allows a detailed acoustic characterization of the impact of the blade design.

Nomenclature

$\boldsymbol{b}$	beamformer output	$\boldsymbol{p}$	complex sound pressure
$\boldsymbol{C}$	cross spectral matrix	Δp_{ts}	total-to-static pressure difference
D	Rotor diameter	$r_{t,m}$	distance focus point to microphone
d_{array}	array aperture	$\dot{V}$	volumetric flow
f	frequency	$\boldsymbol{x}_t$	focus point (3D vector)
$\boldsymbol{h}$	steering vector	η_{ts}	efficiency
k	wave number	Φ	flow-rate coefficient
L_p	sound pressure level	ψ_{ts}	total-to-static pressure coefficient
M	number of microphones	ρ	air density
N	number of focus grid points	τ	torque
n	rotational speed	CSM	cross spectral matrix

I. Introduction

Assessing aeroacoustic phenomena with microphone array methods such as beamforming has become common practice. The main objective applying these methods is to gain information about the location and characteristics of acoustic sources which are emitting simultaneously and in close vicinity of each other. For this, the phase shift of signals recorded synchronously at distributed sensor positions is evaluated with respect to a discretized focus area. This can be done in frequency domain or in time domain.

In time domain, the measured signals are shifted such that the time delay compensates the sound travel time from a chosen focus point to the microphones. The delayed signals are then summed to yield the

*PhD Student, Chair of Technical Acoustics, Brandenburg University of Technology.
†PhD Student, Institute of Process Machinery and Systems Engineering, University of Erlangen-Nuremberg
‡Professor, Chair of Technical Acoustics, Brandenburg University of Technology.

resulting sound pressure for the focus point. This procedure is performed for each focus point so as to gain a map of the source distribution.

In frequency domain, the signals are Fourier-transformed block-wise and their cross-spectra are averaged to obtain the cross-spectral matrix (CSM). The CSM is then multiplied with steering vectors, containing the sound propagation model from focus points to the microphones, which effectively phase-shifts and summates the signals. Existing frequency-domain-based methods usually have a higher capability of distinguishing sources and often calculate faster than methods working in time domain. Furthermore, uncorrelated background noise can be suppressed by the removal of the main diagonal of the CSM for a cleaner source reconstruction.

In principle, evaluations in frequency domain necessitate stationary sources. With moving sources, generally only time domain calculations are possible, since the time delay from source position to receiver changes permanently and cannot be described with a time-invariant steering vector. In the special case of rotating sources, however, it is possible to transform the measured data into a synchronously rotating system, rendering these sources quasi-stationary.[1,2]

The virtual rotating array method is used in this contribution to detect sources occurring on two rotating axial fans, featuring nine forward and backward skewed blades respectively.

II. Materials and methods

A. Experimental setup

Measurements were conducted inside an ISO 5801 standardized inlet test chamber.[3] Different operating conditions of the fans were achieved by varying the inflow of the chamber. The rotation of the fans was kept at a rate of 1500 rpm.

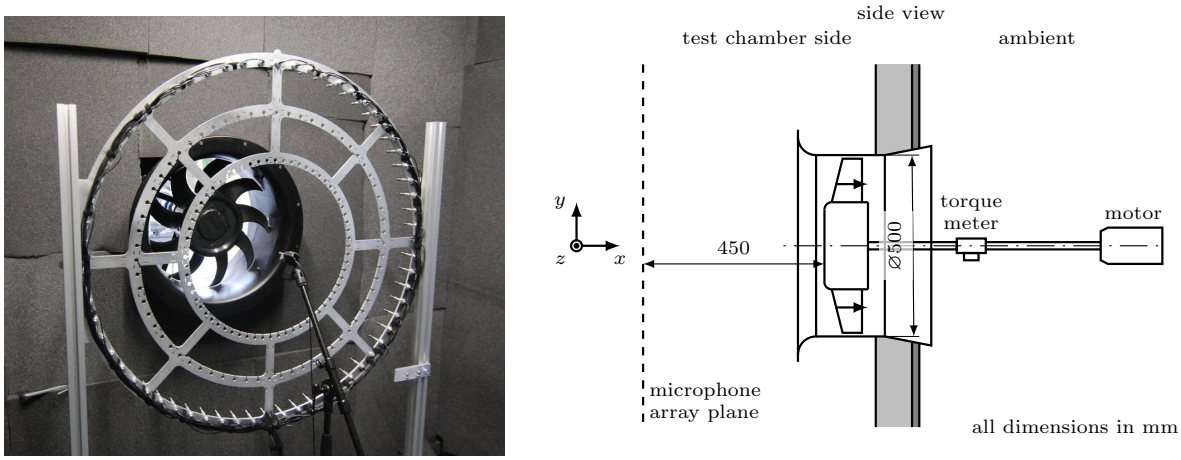

Figure 1. Experimental setup with the microphone array inside the test chamber (left: (fan suction side), right: schematic side view).

The microphone array (Fig. 1) was positioned on the suction side of the fan, at a distance of 0.45 m from the blades. It consists of 64 microphones, arranged evenly in a ring with a diameter of $d_{\text{array}} = 1\,\text{m}$. In addition to the sound pressures, the rotation of the fan is recorded using a trigger-per-revolution signal. The two fans (see Fig. 2) are designed according to the blade element theory for low solidity fans,[4,5] as outlined by Zenger et al.[6]

The fan blades of the forward skewed fan have a varying sweep angle,[7] from 0° at the hub and 55° at the blade tip. Accordingly, the backward skewed fan has a varying sweep angle from 0° at the hub and −55° at the blade tip. Fan design parameters are listed in Table 1. The flow rate coefficient Φ is calculated with

$$\Phi = \frac{4\dot{V}}{\pi^2 D^3 n} \tag{1}$$

Figure 2. Fan with forward skewed blades (left) and backward skewed blades (right). Rotation is clockwise.

and the total-to-static pressure coefficient ψ_{ts} with

$$\psi_{\mathrm{ts}} = \frac{2\Delta p_{\mathrm{ts}}}{\rho\,(D\pi n)^2}\ , \tag{2}$$

where $\dot{V}$ is the volumetric flow, Δp_{ts} is the total-to-static pressure difference and ρ is the air density. With the torque of the fan τ, the efficiency is calculated by

$$\eta_{\mathrm{ts}} = \frac{\dot{V}\Delta p_{\mathrm{ts}}}{2\pi\, n\, \tau}\ . \tag{3}$$

Table 1. Fan design parameters.

Total-to-static pressure coefficient ψ_{ts}	0.18
Flow-rate coefficient Φ	0.18
Number of fan blades	9
Rotational speed n in	$1500\,\mathrm{min}^{-1}$
Fan diameter D in mm	495
Hub diameter in mm	248
Tip gap in mm	2.5
Sweep angle in ° (hub . . . tip)	0 . . . 55, 0 . . . -55

B. Virtual rotating array

With the microphone array centered and aligned with the rotational axis of the fan, the sound pressures can be interpolated so as to simulate an array rotating at the same rate as the fan.[2]

From the recorded trigger-per-revolution signal, the real-time angular position of the fan is calculated. The sound pressures in the rotating domain are then calculated by linearly interpolation of the measured sound pressures between adjacent microphones according to the calculated angles.

C. Beamforming and deconvolution

The virtual rotating data are transformed into frequency domain using Welch's method.[8] The signal is divided into overlapping blocks, onto which an FFT is applied. The resulting complex sound pressures $\boldsymbol{p}$ are cross-correlated and an estimate of the cross-spectral matrix is calculated by averaging the cross-spectra:

$$\boldsymbol{C} = \overline{\boldsymbol{p}\boldsymbol{p}^{\mathrm{H}}}\ . \tag{4}$$

The superscript $^{\mathrm{H}}$ denotes the Hermitian transpose.

The classic delay-and-sum beamformer formulation in the frequency domain is

$$b(\boldsymbol{x}_t) = \boldsymbol{h}^{\mathrm{H}}(\boldsymbol{x}_t)\, \boldsymbol{C}\, \boldsymbol{h}(\boldsymbol{x}_t)\ , \qquad t = 1 \ldots N\ . \tag{5}$$

N denotes the number of arbitrary focus points $\boldsymbol{x}_t$, at which this equation is to be evaluated. For the case at hand, sound pressures are evaluated on a three-dimensional focus grid, fully encompassing the area of the fan. With the multiplication of the steering vector $\boldsymbol{h}$, a summation of the phase-shifted signals is achieved, according to the distances from the M microphones to the N focus points. Assuming a monopole sound propagation model, its entries can be calculated via[9]

$$h_m = \frac{1}{r_{t,0} r_{t,m} \sum_{l=1}^{M} {r_{t,l}}^{-2}}\, \mathrm{e}^{-\mathrm{j}k(r_{t,m} - r_{t,0})}\ , \qquad m = 1 \ldots M\ . \tag{6}$$

The result obtained by evaluating Eq. (5) features artifacts due to the array geometry, the chosen focus grid, and the source characteristics not perfectly represented by the sound propagation model. Applying the CLEAN-SC algorithm,[10] the original map can be deconvoluted by identifying correlated portions of the classic beamformer output.

Important measurement and data processing parameters are summarized in Table 2.

Table 2. Data acquisition and processing parameters.

Number of microphones	64
Diameter of ring array	1 m
Distance from fan to array	0.45 m
Measurement time	30 s
Sampling rate	48 kHz
FFT block size	2048 samples
FFT window	von Hann
	50% overlap
Circular focus grid	$r_{\min} = 0.1$ m, $r_{\max} = 0.35$ m
	$x_{\min} = 0.45$ m, $x_{\max} = 0.55$ m
Resolution of focus grid	$\Delta yz = 0.01$ m, $\Delta x = 0.02$ m
CLEAN-SC iterations	500
CLEAN-SC damping	0.6

III. Results

The aerodynamic characteristic curves for both fans are shown in Figure 3. Above the design flow rate coefficient of $\Phi = 0.18$, the fans have similar pressure coefficients. At lower flow rate coefficients, the forward skewed fan has an extended operating range,[7,11] i. e. a significantly higher total-to-static pressure coefficient. Below a flow rate coefficient of $\Phi = 0.1$, the fans are operated in the deep stall region, where the backward skewed fan tends to have higher pressure coefficients. At the design point and lower flow rate coefficients up to $\Phi = 0.1$, the forward skewed fan has a higher total-to-static efficiency.

Sound maps are evaluated for three different flow rate coefficients: At $\Phi = 0.22$, the fans are operating beyond their design point, thus the fan blades are mildly loaded. At the design point at $\Phi = 0.18$, the fans are close to their maximal achievable pressure rise and the fan blades are highly loaded. As mentioned, at $\Phi = 0.105$, the fan is in the deep stall region, i. e. flow separations close to the fan blade leading edges can be expected.

Sound maps for the three flow rate coefficients in the 5 Khz one-third octave band are shown in Figure 4. A clear repetitive pattern can be seen in all cases, corresponding to the nine fan blades. At the lowest flow rate coefficient of $\Phi = 0.105$, major sound sources on the forward skewed fan can be found along the whole leading edge. This can be caused by flow separations in this region. In contrast, sources on the backward skewed fan are found both on the leading edges and the blade surfaces and mostly at higher radii, where higher flow speeds occur. Thus, at low flow rate coefficients, backward skewed fan blades seem to stabilize

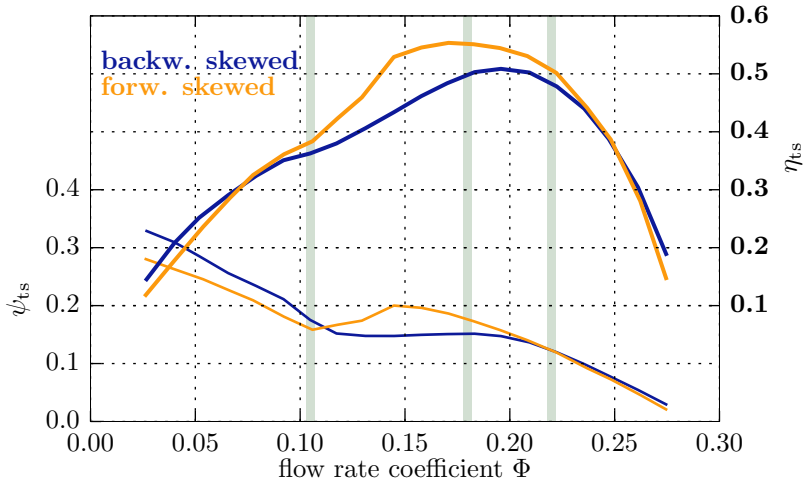

Figure 3. Pressure coefficient ψ_{ts} and efficiency η_{ts} for different flow rate coefficients Φ and the forward and backward skewed fan. The light-green lines mark the coefficents for which the soundmaps in Fig. 4 are evaluated.

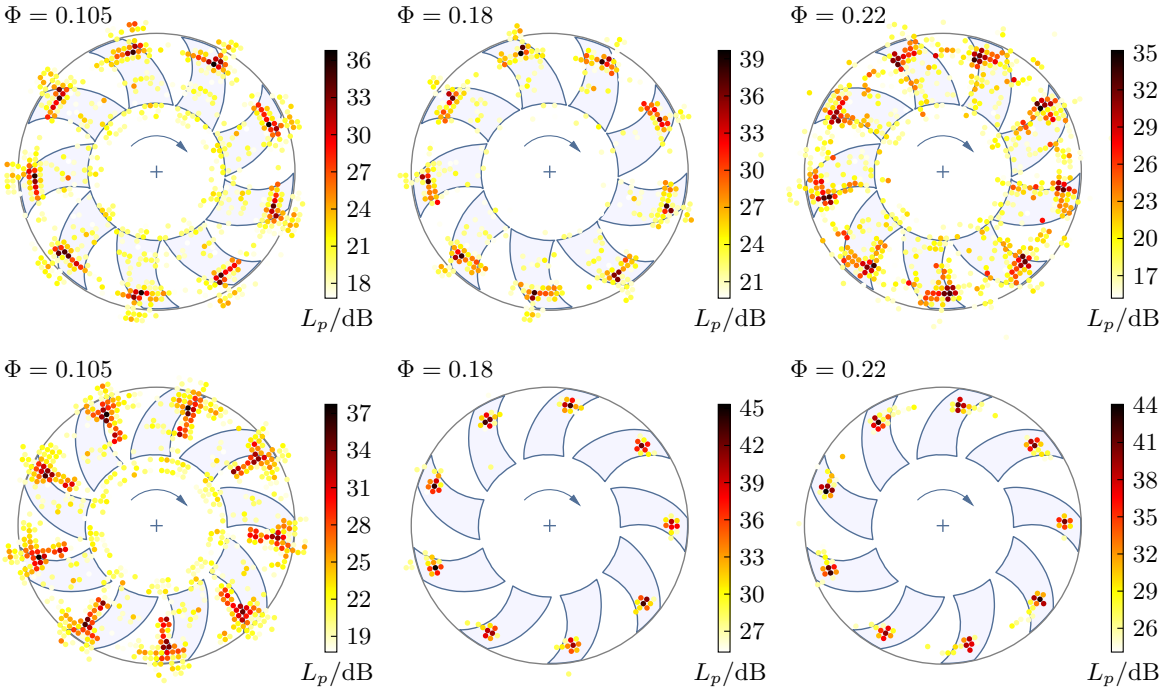

Figure 4. Soundmaps for the 5 kHz one-third octave band for different operating conditions of the two fans.

the flow as sources do not solely occur on the fan blade leading edges, which would indicate major flow separations due to stalling.

At $\Phi = 0.18$, sources on the forward skewed fan are located near the fan blade leading edges. As no flow separations are expected at this flow rate coefficient, this can be caused by turbulent ingestion noise, i. e. sound generated by the interaction of the fan blade leading edges with the inflow. Although the fans were operated under free inflow conditions, there is still a base turbulence intensity, which can account for this effect. Turbulent inflow statistics, measured with a laser Doppler anemometer can be found in Zenger et al.[12] This mechanism seems to be of minor importance on the backward skewed fan as sources can be found on the blade surfaces and to some extent on the blade leading edges. Sources on the blade surfaces can be induced by pressure fluctuations under the turbulent boundary layer.[5]

At a flow rate coefficient of $\Phi = 0.22$, sources on the forward skewed fan are again located near the fan blade leading edges. In contrast, sources on the backward skewed fan can be found on the fan blade trailing edges, indicating trailing edge noise due to flow separation.

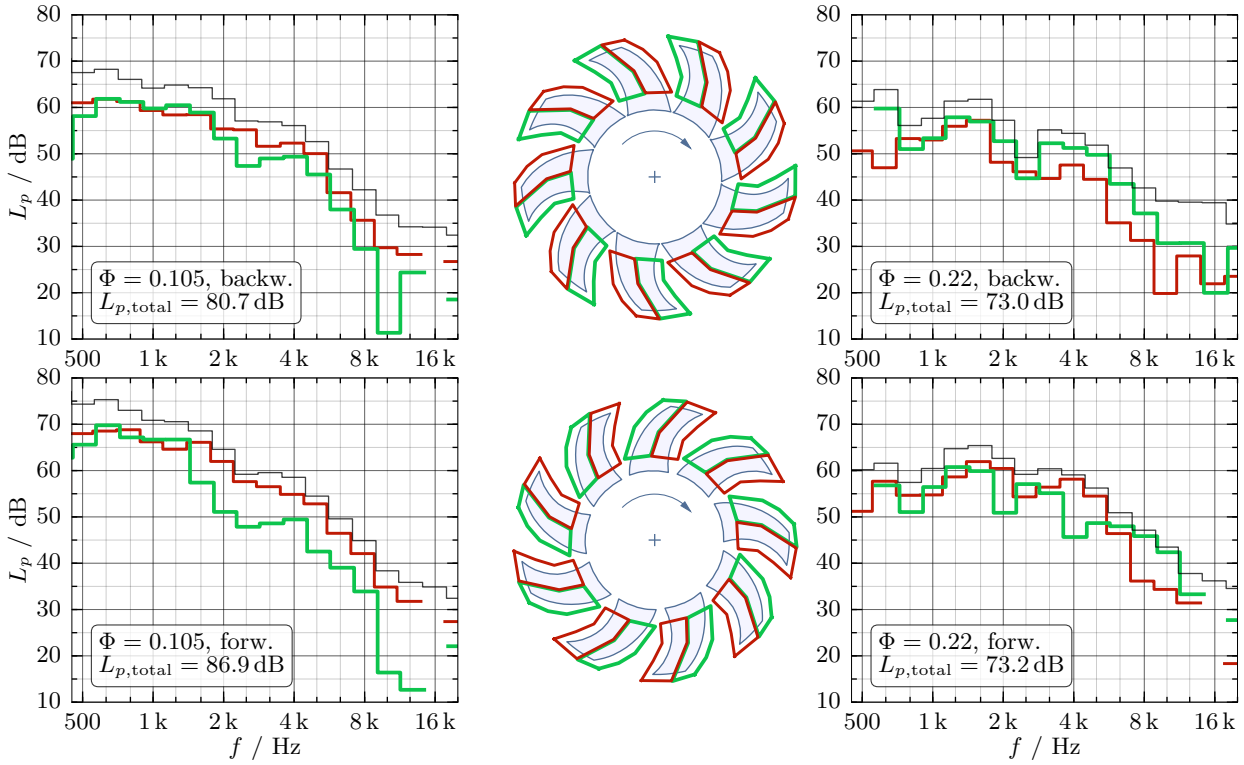

Figure 5. One-third octave spectra integrated over the leading and trailing edge sub-regions of the fans for two different flow rate coefficients. The spectra summed over the whole focus area are also shown for reference (black curve), as is the total sound pressure level for each case.

Integrated spectra for the lowest and highest considered flow rate coefficient are shown in Figure 5. At $\Phi = 0.105$, less noise is emitted from the trailing edges than from the leading edges for both fans. However, in case of the forward skewed fan, the dominant leading-edge noise is more distinct with levels of 10 dB above trailing edge noise for several bands. As was already observed in the sound maps, for the backward skewed fan, the sources are more evenly distributed over the chord. Mostly due to the sources on the leading edge, the overall sound pressure level of the forward skewed fan is 6 dB higher than that of th backward skewed fan for this operating point.

While at $\Phi = 0.22$, the overall sound pressure level is of the same order of magnitude for both fans, the leading and trailing edge spectra differ considerably. The trailing edges of the backward skewed fan feature higher levels for the most part of the spectrum above $f \geq 2\,\mathrm{kHz}$. In contrast, leading edge noise seems to be more important for the forward skewed fan for frequencies up to $f < 6.3\,\mathrm{kHz}$.

IV. Conclusion

The microphone array method for detecting rotating sources has been successfully applied to analyze noise emissions on skewed fans. In contrast to a single spectral curve as derived from single-microphone measurements, with the presented method it is possible to localize different source mechanisms and discern the spectral characteristics, e.g. of the leading and trailing edges of the fans. Furthermore, the method allows to analyze the variation of these characteristics with changing operating point.

Most prominently, the leading edge noise is dominant for both fans at a low volumetric flow rate, while trailing edge noise becomes more important at higher flow rates. As has been shown, the shift from leading edge to trailing edge noise occurs at different frequencies, depending on the fan. Moreover, the spectral characteristics of the sub-components differ depending on the geometry.

The presented method not only proves that sound emission can be substantially changed by the blade design, but also provides a tool to characterize the acoustic impact of design changes.

References

[1]Dougherty, R. P. and Walker, B. E., "Virtual Rotating Microphone Imaging of Broadband Fan Noise," *Proceedings of the 15th AIAA/CEAS Aeroacoustics Conference*, 2009.

[2]Herold, G. and Sarradj, E., "Microphone array method for the characterization of rotating sound sources in axial fans," *Noise Control Engineering Journal*, Vol. 63, No. 6, 2015, pp. 546–551.

[3]ISO, "ISO 5801 (2007-12) – Industrial fans – Performance testing using standardized airways," 2007.

[4]Pfleiderer, C. and Petermann, H., *Strömungsmaschinen*, Springer-Verlag Berlin Heidelberg, 2005.

[5]Carolus, T., *Ventilatoren – Aerodynamischer Entwurf, Schallvorhersage, Konstruktion*, Vieweg+Teubner Verlag, 2003.

[6]Zenger, F., Junger, C., Kaltenbacher, M., and Becker, S., "A benchmark case for aerodynamics and aeroacoustics of a low pressure axial fan," *SAE Technical Paper 2016-01-1805*, 2016.

[7]Vad, J., *Blade Sweep Applied to Axial Fan Rotors of Controlled Vortex Design*, Ph.D. thesis, Hungarian Academy of Sciences, 2011.

[8]Welch, P. D., "The Use of Fast Fourier Transform for the Estimation of Power Spectra: A Method Based on Time Averaging Over Short, Modified Periodograms," *IEEE Transactions on Audio and Electroacoustics*, Vol. 15, No. 2, 1967, pp. 70–73.

[9]Sarradj, E., "Three-Dimensional Acoustic Source Mapping with Different Beamforming Steering Vector Formulations," *Advances in Acoustics and Vibration*, Vol. 2012, 2012, pp. 1–12.

[10]Sijtsma, P., "CLEAN based on spatial source coherence," *International Journal of Aeroacoustics*, Vol. 6, No. 4, dec 2007, pp. 357–374.

[11]Corsini, A. and Rispoli, F., "Using Sweep to Extend the Stall-Free Operational Range in Axial Fan Rotors," *Proceedings of the Institution of Mechanical Engineers, Part A: Journal of Power and Energy*, Vol. 218, No. 3, 2004, pp. 128–139.

[12]Zenger, F., Herold, G., and Becker, S., "Acoustic Characterization of Forward- and Backward-Skewed Axial Fans under Increased Inflow Turbulence," *Proceedings of the 22nd AIAA/CEAS Aeroacoustics Conference*, Lyon, France, 2016.